Received: 18 June 2022 | Revised: 23 September 2022 | Accepted: 5 October 2022

DOI: 10.1002/alz.12850

Alzheimer's & Dementia®
THE JOURNAL OF THE ALZHEIMER'S ASSOCIATION

RESEARCH ARTICLE

A structural and resting-state functional connectivity investigation of the pulvinar in elderly individuals and Alzheimer's disease patients

Halil Aziz Velioglu[1,2] | **Behcet Ayyildiz**[3,4] | **Sevilay Ayyildiz**[3,4] | **Bernis Sutcubasi**[5] | **Lutfu Hanoglu**[2,6] | **Zubeyir Bayraktaroglu**[2,7] | **Burak Yulug**[8]

[1]Science for Life Laboratory, Department of Women's and Children's Health, Karolinska Institute, Stockholm, Sweden

[2]Functional Imaging and Cognitive-Affective Neuroscience Lab (fINCAN), Health Sciences and Technology Research Institute (SABITA), Regenerative and Restorative Medicine Research Center (REMER), Istanbul Medipol University, Istanbul, Turkey

[3]Anatomy PhD Program, Graduate School of Health Sciences, Kocaeli University, Kocaeli, Turkey

[4]Department of Anatomy, School of Medicine, Istinye University, Istanbul, Turkey

[5]Department of Psychology, Faculty of Arts and Sciences, Acibadem University, Istanbul, Turkey

[6]Department of Neurology, School of Medicine, Istanbul Medipol University, Istanbul, Turkey

[7]Department of Physiology, Istanbul Medipol University, International School of Medicine, Istanbul, Turkey

[8]Alanya Alaaddin Keykubat University, School of Medicine, Alanya/Antalya, Turkey

Correspondence
Burak Yulug, Alanya Alaaddin Keykubat University, School of Medicine, Alanya/Antalya, Turkey.
E-mail: burakyulug@gmail.com

Abstract

In Alzheimer's disease (AD), structural and functional changes in the brain may give rise to disruption of specific cognitive functions. The aim of this study is to investigate the functional connectivity alterations in the pulvinar's subdivisions and total pulvinar voxel-based morphometry (VBM) changes in individuals with AD and healthy controls. A seed-based functional connectivity analysis was applied to the anterior, inferior, lateral, and medial pulvinar in each hemisphere. Furthermore, VBM analysis was carried out to compare gray matter (GM) volume differences in the pulvinar and thalamus between the two groups. Connectivity analysis revealed that the pulvinar subdivisions had decreased connectivity in individuals with AD. In addition, the pulvinar and thalamus in each hemisphere were significantly smaller in the AD group. The pulvinar may have a role in AD-related cognitive impairments and the intrinsic connectivity network changes and GM loss in pulvinar subdivisions suggest the cognitive deterioration occurring in those with AD.

KEYWORDS
Alzheimer's disease, cognitive impairment, functional magnetic resonance imaging, pulvinar, thalamus, voxel-based morphometry

Highlights

- The pulvinar may play a role in pathophysiology of cognitive impairments in those with Alzheimer's disease (AD).
- Decreased structural volume and functional connectivity were found in patients with AD.
- The inferior pulvinar is functionally the most affected subdivision by AD compared to the others.

Halil Aziz Velioglu and Behcet Ayyildiz contributed equally to this work and share first authorship.

1 | NARRATIVE

1.1 | Contextual background

Structural and functional changes in the brain at the macroscopic level are observed shortly after neuronal damage at the microscopic level, characterized by protein depositions in numerous brain areas, subsequently causing further brain volume loss.[1–5] This is consistent with longitudinal data from Alzheimer's disease (AD) patients showing widespread loss of brain volume particularly affecting the gray matter (GM) and contributing directly to impaired cognitive function as confirmed by anatomical-weighted magnetic resonance imaging (MRI) scans and several cognitive tests.[2] However, specific cognitive functions including attention and executive function are associated not only with temporohippocampal functions, but also with other regions, such as the thalamus, involved in a number of specific attention and executive cognitive functions.[6,7] One good example of this is the role of the thalamus in cognition in the elderly population, although its role is rarely mentioned in neuroimaging studies of AD patients.[8,9] This may be due to methodological differences between studies and overfocus on conventional anatomical regions obstructing the identification of other brain regions, such as the thalamus, involved in AD.

The pulvinar, which is the largest nucleus of the thalamus in primates, was firstly described by Cajal in 1911 as a "visual pulvinar" According to Cajal, the pulvinar is more developed in primates while it is absent in rodents and other many creatures.[10] A recent study showed that the pulvinar makes up 30% of thalamus volume in primates and humans and occupies a much smaller size in rodents' thalamus volume[11] suggesting that the pulvinar is well developed in higher mammals, particularly in humans and primates, compared to the other creatures.[12]

The pulvinar is cytoarchitectonically subdivided into the anterior pulvinar (PuA), inferior pulvinar (PuI), medial pulvinar (PuM), and lateral pulvinar (PuL) exerting strong connectivity with various cortical areas, including the visual cortex and several heteromodal association and limbic areas leading to its consideration as a thalamic associative nucleus.[13,14] The pulvinar receives the most divergent inputs from the cortex and sends related efferents to it,[15] creating an extensive and reciprocal connectivity between the pulvinar and cortical areas. Several studies show that these abovementioned widespread connections of the pulvinar may contribute to advanced cognitive,[16,17] emotional,[18,19] and somatosensory[20] capabilities. This was confirmed with several diffusion tensor imaging (DTI) studies showing strong connections of the pulvinar with prefrontal, posterior parietal, inferior temporal association areas; frontal eye fields; visual cortical areas (V1, V2, V3, V4, and V5); superior colliculus; posterior parietal cortex; primary motor cortex; dorsal prefrontal cortex; orbitofrontal cortex; and caudate nucleus.[21] Also, task-based functional magnetic resonance imaging (fMRI) studies determined that the pulvinar contributes to several attention functions, attributing a special role to PuM depending on the task performed.[22] In line with this, the connections between the PuM and the posterior parietal, inferior temporal, cingulate, retrosplenial, and prefrontal cortical areas have been directly associated with directed attention, executive functions, and working memory.[23,24] Similarly, the PuI and PuL, known as the "visual pulvinar",[25,26] exhibit strong network connections with visual cortical areas, including the occipital, temporal, and parietal lobes through critical subcortical components of the dorsal and ventral stream of visual cortical processing.[27] Based on these unique anatomical and functional properties, lesions in the pulvinar can dramatically impair several attentional, visuomotor, and emotional processes. For instance, unilateral lesions of the pulvinar result in a contralateral neglect syndrome resembling that resulting from lesions of the posterior parietal cortex. Additionally, patients with pulvinar lesions have encoding deficits of spatial information leading to difficulty in filtering of distracting information.[28,29] Moreover, the pulvinar supports the attentional process by distinguishing between contextually relevant and irrelevant somatosensory stimuli and coordinating multimodal signals due to its connection with association cortices.[30] Hence, relevant lesions might lead to several spatial and temporal attention deficits.[31] Additionally, motor deficits occur by the loss of integrative pulvinar connections. Wilke et al. observed reach and grasp deficits after selective pulvinar lesion in humans suggesting the role of PuM in motor planning of voluntary actions.[32] Taken together, based on its strong connectivity with various cortical areas, including the visual cortex and several heteromodal association and limbic areas, the pulvinar represents a novel subcortical prototypical associative center. For instance, with its participation in heavy dynamic interconnections, the pulvinar might make the right hemisphere especially important in lateralization in spatial coding of object position. Similarly, based on its reciprocal connections with the amygdala and inferotemporal cortex, containing face-selective neurons, complete

RESEARCH IN CONTEXT

1. **Systematic Review**: The authors reviewed the literature using traditional (e.g., PubMed) sources. The pulvinar is the largest nucleus of the thalamus and has extensive connections with multimodal cortical areas. However, the effects of the pulvinar are poorly understood in Alzheimer's disease (AD), and it is unclear if decreased pulvinar connectivity influences cognition during the pathophysiology of AD.
2. **Interpretation**: Our study increases knowledge about function of the pulvinar, and especially alteration of its volume and functional connectivity in AD. The changes in the pulvinar in those with AD has the potential to help interpret mechanisms of cognitive impairment.
3. **Future Directions**: These findings highlight the need to consider that structural and functional alteration of the pulvinar may play a critical role in the pathophysiology of AD. Task-based functional magnetic resonance imaging studies could help examine our inference about altered pulvinar connectivity in AD.

unilateral loss of the pulvinar might led to considerable difficulties in recognizing fearful facial expressions, and face orientation. In short, the pulvinar facilitates a large attention-related communication network system including both sensory and higher-order cortices, by coordinating their interactions in the temporal domain to maintain the function of key arousal and cognitive networks.

The purpose of this study was to evaluate functional and volumetric changes in the pulvinar in AD patients and healthy controls using resting-state fMRI (rs-fMRI) and T1-weighted MRI scans. To the best of our knowledge, this is the first study directly investigating structural volumes in the pulvinar along with functional connectivity of the PuA, PuI, PuL, and PuM subdivisions in both AD and healthy controls.

1.2 | Study conclusions and disease implications

Decreased volumes were observed in the pulvinar, a region that was believed to be not typically related to cognitive function or AD. However, both longitudinal studies and neuropathological models, such as Braak's staging, indicate that the pulvinar is an important area affected by neurofibrillary tangles.[26] This is consistent with several neuroanatomical studies demonstrating noticeable connections between the pulvinar and cognitive brain regions involved in cognition and AD in both humans and animals.[10,33] For instance, one recent study indicated the role of ventral thalamic GM degeneration in cognitive impairment in AD.[8] Additionally, specific abnormalities of the pulvinar region were linked to Lewy body dementia associated with special cognitive impairments involving attention, and visuospatial and memory processes.[34,35] Briefly, our results suggest the pulvinar may play a role in AD-related cognitive impairment which, together with other critical regions, was affected in this study, and may contribute to cognitive deficits.

Interestingly, the largest volume reductions in the pulvinar indicate a divergent role of the pulvinar in executive functions, visual attention, and working memory.[7,16,18] Although global differences were observed in AD-related GM volumes, the pulvinar region remained significantly affected in AD dementia at the < 0.01 level. Based on the previous literature suggesting that thalamic AD-related volumetric reductions are not uniform,[36] we have obtained age-corrected values. Additionally, we performed correlation analysis between ages and imaging results (time series) separately in the control and AD groups. After accounting for the age differences between the groups, we have observed no significant changes in the structural and functional data, which was also suggested with our correlation analysis in separated groups.

The connectivity of the pulvinar in non-human primates has been well described with its diverse connections with cortical and subcortical regions. These non-human neuroanatomical studies reported that the pulvinar is interconnected with the prefrontal cortex, posterior cingulate cortex, inferior temporal gyrus, inferior parietal lobule, insular cortex, visual cortical areas, amygdala, superior colliculus, pons, and putamen, highlighting the role of the pulvinar as a multimodal integration center.[23,26,37] In our study the general connectivity pattern is consistent with studies shown in monkeys and our rs-fMRI data represent a considerable fraction shown in the previous monkey studies.

In our study, we found a considerable asymmetry between left and right pulvinar connectivity (Tables 1 and 2). This is in line with the previous study by Cotton and Smith indicating a greater activation in the left pulvinar than the right side associated with greater activation suggesting the role of the functional laterality of the pulvinar[38] in attentional processes. Furthermore, although anatomical pulvinar connections are symmetrical, laterality of parietal function coupled with parietal interconnections with the pulvinar[39] may result in asymmetric pulvinar activity.[38]

Also, our functional data suggested the role of the pulvinar in AD. Similar to our previous Parkinson's disease study, in which decreased functional connectivity was observed in patients, and which attributed a special role of the pulvinar in social integration and motor movements (unpublished data) altered functional connectivity was determined in AD patients in the present study. Our observation of significant functional alterations in the AD group may suggest that thalamic network function may be prominent during the progression to late AD stages where also other regions degenerate to a similar degree. More specifically, our findings of significant functional differences between healthy controls and patients with AD may suggest that decreased thalamic network function may be seen in the early dementia stages, after which progression to late stages occurs, in which other regions also degenerate to a similar degree.

The results of this study are generally in line with recent cognitive data showing that posterior thalamic atrophy may be a predictor of cognitive decline and therefore a game-changer region in dementia, in addition to late-degenerated hippocampal regions.[2,40-42] Evidence for this is provided by our finding that cognitive rates of change are correlated with concurrent changes in structural and functional pulvinar parameters, yielding a strong clinical message that posterior thalamic degeneration may play a pivotal role in cognitive impairment. The present research identified the pulvinar structurally and functionally affected region in AD and confirmed previous reports of the contribution of the pulvinar to attention, executive function, and working memory.[20]

In sum, this study provides additional structural insight into the cognitive deterioration occurring in AD and proposes an additional role of the (posterior) thalamus in the cognitive deterioration that characterizes AD, which may eventually be of assistance in the prognosis and treatment of disease progression.

1.3 | Study limitations and recommendations for future studies

This article provides information about the pulvinar nucleus, which has not received the attention it deserves, in the pathophysiology of AD. This study is limited by our inability to evaluate all participants' motor, cognitive, and mood performance in detail. Such information may be particularly useful for clarifying the functional and structural changes in the specific pulvinar nuclei in AD. On the other hand, the current

TABLE 1 Clusters of within-group functional connectivity for the left hemisphere seeds

Region	Peak MNI coordinates (x, y, z)	Size	Size- pFWE	t-Max	Region	Peak MNI coordinates (x, y, z)	Size	Size- pFWE	t-Max
Healthy control					**Alzheimer's disease**				
L-anterior pulvinar									
L-R thalamus	−12, −22, 08	1189	0.000000	13.07	R-L thalamus, L- putamen	−12, −22, 08	2433	0.000000	13.43
L-fusiform cortex, L-ITG, L-PPHG	−34, −32, −16	255	0.000211	7.27					
PCC, precuneus cortex	02, −54, 10	250	0.000247	6.68					
L-inferior pulvinar									
L-R thalamus, L-R hippocampus	−18, −30, 00	1686	0.000000	17.44	R-L thalamus, PCC, R-L hippocampus Precuneus cortex, R-L lingual gyrus	−20, −32, 00	2642	0.000000	12.19
L- ITG, L-fusiform cortex	−46, −48, −22	139	0.007013	6.86	R-insular cortex, R- IFG pars opercularis	46, 08, 04	519	0.000000	−7.76
					R-SFG, R-L SMC	04, 08, 64	439	0.000001	−6.97
					L- fusiform cortex, L-ITG, L-cerebellum	−40, −38, −26	437	0.000001	6.51
L-lateral pulvinar									
L-R thalamus	−12, −22, 14	1369	0.000000	13.95	R-L thalamus, L-putamen, L-insular cortex	−16, −26, 12	2120	0.000000	11.54
Precuneus cortex, L-R LOC, L-SPL	14, −76, 50	571	0.000000	8.66					
FMC	−46, 44, −16	455	0.000000	−9.71					
R-amygdala	14, 02, −16	150	0.004708	−6.84					

(Continues)

TABLE 1 (Continued)

Region	Peak MNI coordinates (x, y, z)	Size	Size- pFWE	t-Max	Region	Peak MNI coordinates (x, y, z)	Size	Size- pFWE	t-Max
Healthy control					**Alzheimer's disease**				
L-medial pulvinar									
L-R thalamus, PCC	−12, −30, 06	3063	0.000000	18.23	R-L thalamus, PCC	−10, −28, 14	3570	0.000000	22.54
ACC, R-PreCG, R-L paracingulate gyrus	42, 02, 44	905	0.000000	−8.77	L-R PreCG, L-PostCG, L-SMC, ACC	−42, −20, 48	834	0.000000	−8.99
R-L SMG	62, −24, 36	474	0.000000	−9.15	R-MFG	38, −04, 16	419	0.0000004	−7.32
Precuneus cortex	06, −46, 36	384	0.000003	6.87	R-IFG, R-insular cortex	36, 06, 16	367	0.0000016	-8-.95
R-lingual gyrus, R-ICC	10, −86, 02	338	0.000012	−8.22	R-L ICC, R-SCC	−10, −70, 06	216	0.0001177	−5.91
R-MTG, R-fusiform cortex	36, −14, −24	319	0.000022	9.87					
L-SFG, L-MFG	−28, 24, 52	301	0.000037	10.37					
R-LOC	10, −64, 60	281	0.000069	−6.50					
R-cerebellum	30, −60, −26	178	0.002133	−13.39					

Abbreviations: ACC, anterior cingulate cortex; FMC, frontal medial cortex; FWE, family-wise error; ICC, intracalcarine cortex; IFG, inferior frontal gyrus; ITG, inferior temporal gyrus; L, left; LOC, lateral occipital cortex; MFG, middle frontal gyrus; MNI, Montreal Neurological Institute; MTG, middle temporal gyrus; PCC, posterior cingulate cortex; PostCG, postcentral gyrus; PPHG, posterior parahippocampal gyrus; PreCG, precentral gyrus; R, right; SCC, supra calcarine cortex; SFG, superior frontal gyrus; SMC, supplementary motor cortex; SMG, supramarginal gyrus; SPL, superior parietal lobule.

TABLE 2 Clusters of within-group functional connectivity for the right hemisphere seeds

Region	Peak MNI coordinates (x, y, z)	Size	Size- pFWE	t-Max	Region	Peak MNI coordinates (x, y, z)	Size	Size-pFWE	t-Max
Healthy control					**Alzheimer's disease**				
R-anterior pulvinar									
L-R thalamus, R- insular cortex	10, −20, 10	1673	0.000000	15.81	R-L thalamus, R-L putamen, R-insula cortex, R-pallidum	12, −22, 10	2495	0.000000	10.29
ACC	08, 20, 32	205	0.000787	7.28	Precuneus cortex, R-L LOC, R-angular gyrus	−12, −78, 44	1043	0.000000	7.31
					L-caudate	−18, 10, 20	243	0.000584	−7.19
R-inferior pulvinar									
R-L thalamus, L-R hippocampus, PCC	16, −28, 00	1136	0.000000	14.93	R-L thalamus, PCC, precuneus cortex, R-L hippocampus, Brainstem, L-lingual gyrus	20, −30, 00	2541	0.000000	15.58
Precuneus cortex	02, −64, 24	524	0.000000	5.60	L-R fusiform cortex, L-R cerebellum	−36, −38, −26	451	0.000001	8.31
L- MFG	−30, 36, 24	183	0.001604	−7.50					
R-lateral pulvinar									
L-R thalamus	12, −22, 14	1315	0.000000	11.15	R-L thalamus	16, −24, 10	1673	0.000000	10.28
Precuneus cortex	−02, −42, 50	246	0.000356	7.51	R-L SMG, R-L SPL	38, −52, 46	506	0.000000	7.57
					PCC	−02, −28, 40	433	0.000002	7.78
					L-PreCG	−08, −20, 70	168	0.004834	6.35
					R-cerebellum	22, −48, −38	168	0.004834	6.82
					R-MTG	58, −46, −10	164	0.005555	7.70

(Continues)

TABLE 2 (Continued)

Region	Peak MNI coordinates (x, y, z)	Size	Size- pFWE	t-Max	Region	Peak MNI coordinates (x, y, z)	Size	Size-pFWE	t-Max
Healthy control					**Alzheimer's disease**				
R-medial pulvinar									
L-R thalamus, PCC	10, −26, 08	3719	0.000000	17.65	L- R thalamus, PCC	10, −26, 10	3690	0.000000	19.26
Brainstem	12, −16, −26	830	0.000000	9.55	L-R PreCG,L-R PostCG, L-R SMC	−44, −02, 50	1945	0.000000	−9.19
R-SMG	54, −34, 28	459	0.000001	−9.01	L-R ICC	−10, −74, 08	563	0.000000	−6.36
L-insular cortex	−36, −04, −12	458	0.000001	−9.68					
L-R ICC, L-R lingual gyrus	06, −64, 08	395	0.000003	−7.30					
R-L IFG, R-L PreCG	42, 04, 18	340	0.000015	−7.72					
L-R cerebellum	06, −50, −46	312	0.000033	8.37					
R-hippocampus, R-fusiform cortex	36, −14, −24	280	0.000087	9.00					
ACC, PCC	−02, −12, 38	200	0.001145	6.58					
L-MFG	−46, 02, 46	187	0.001793	−6.27					
R-PostCG	08, −28, 72	170	0.003275	8.93					
R-SPL, R-angular gyrus	42, −48, 54	158	0.005070	−6.07					

Abbreviations: ACC, anterior cingulate cortex; FWE, family-wise error; ICC, intracalcarine cortex; IFG, inferior frontal gyrus; ITG, inferior temporal gyrus; L, left; LOC, lateral occipital cortex; MFG, middle frontal gyrus; MNI, Montreal Neurological Institute; MTG, middle temporal gyrus; PCC, posterior cingulate cortex; PostCG, postcentral gyrus; PreCG, precentral gyrus; R, right; SMC, supplementary motor cortex; SMG, supramarginal gyrus; SPL, superior parietal lobule.

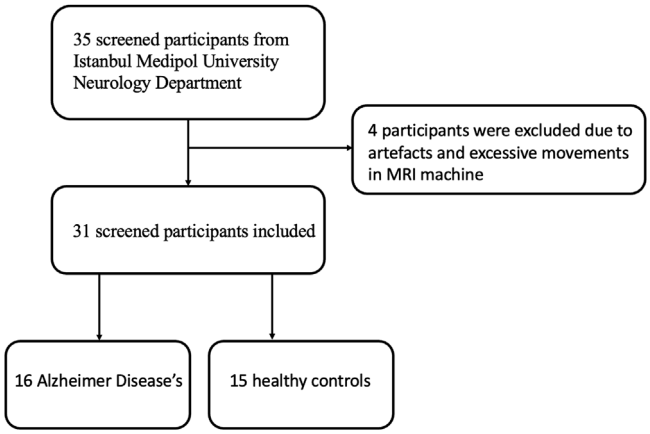

FIGURE 1 Flowchart of the study showing the participants' acceptance. MRI, magnetic resonance imaging

study had a small sample size and such studies conducted in a large population would be better to address the role of the pulvinar in AD. Despite these minor limitations, the precise role of the pulvinar in AD remains to be elucidated and further studies are needed. Although rs-fMRI provides an excellent opportunity to investigate the connectivity of the pulvinar in AD patients, the role and contribution of the pulvinar to AD would be better identified in task-based fMRI studies involving specific tasks that assess motor, cognitive, and social functions.

2 | METHODS

2.1 | Participants

Sixteen individuals diagnosed with AD and 15 healthy controls, who had no neurological disease and traumatic history, were included in the present study (Figure 1). All participants completed a medical history and physical examination and underwent structural imaging and rs-fMRI. Mini Mental State Examination (MMSE) was used as the global cognitive assessment. All AD patients had mild to severe AD symptoms (Clinical Dementia Rating ≥ 1). The Istanbul Medipol University ethical committee approved the present study (Ethical Report: E-10840098-772.02-6112-E. 1139).

2.2 | Imaging acquisition

The rs-fMRI and T1-weighted anatomical images were acquired in a Philips Achieva 3 Tesla scanner (Philips Medical Systems). The T1-weighted images were obtained with following parameters: 190 slices, field of view (FOV) = 256 × 256 × 190 mm, voxel size = 1 × 1 × 1 mm, repetition time (TR) = 8.1 ms, echo time (TE) = 3.7 ms, flip angle = 8°. The rs-fMRI scans were obtained by a T2-weighted gradient-echo echo-planar imaging (GE-EPI) sequence with the following parameters: TR 2230 ms, TE 30 ms, 300 volumes, 35 axial slices, FOV = 240 × 240 × 140 mm, voxel size = 3 × 3 × 4, flip angle 77, with a duration 12 minutes. The participants were requested to keep their eyes open and not move their heads during the scan to get a good quality resting image.

2.3 | rs-fMRI data processing

The seed-based resting-state functional connectivity analysis was processed using functional connectivity toolbox v18 (CONN; http://web.mit.edu/swg/software.htm) running under Statistical Parametric Mapping 12 (SPM12; http://www.fil.ion.ucl.ac.uk/spm/software/spm12/), in MATLAB 20b version (MathWorks).[44] The preprocessing pipeline involves the following steps: realignment and unwarping, slice-timing correction, structural segmentation and normalization, functional normalization, outlier identification, and functional smoothing. Functional images of each participant were realigned to account for head movements. Previous studies have explored that realignment is not sufficient to remove motion artefacts, and that head movements can impact functional connectivity results.[44,45] Thus, artefact removal tools (ART) were used to scrub outlier scans for functional images.[47] Participant head movement realignment and scrubbing parameters (using the conservative setting with 95th percentiles with linear motion parameters > 0.5 mm and global-signal z > 3 value threshold) were assigned

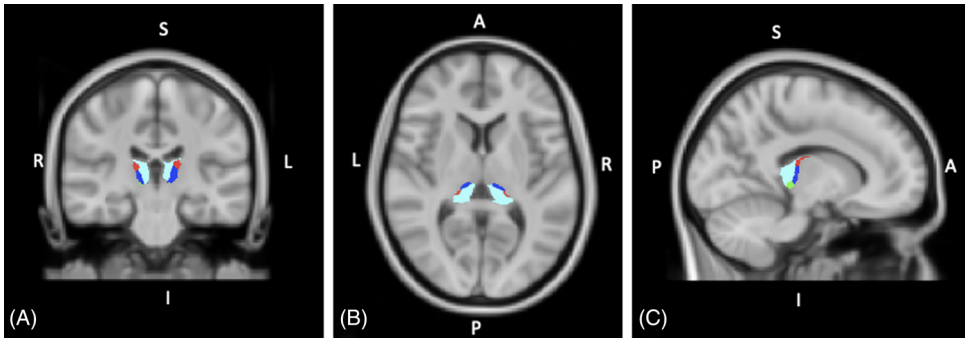

FIGURE 2 Coronal (A), axial (B), and sagittal (C) sections of an MNI_152 template showing the pulvinar nucleus seeds. Eight seeds were generated by FreeSurfer thalamic segmentation of the MNI_152 template. The anterior pulvinar, inferior pulvinar, lateral pulvinar, and medial pulvinar are blue, green, red, and light blue colors in both hemispheres, respectively. MNI, Montreal Neurological Institute

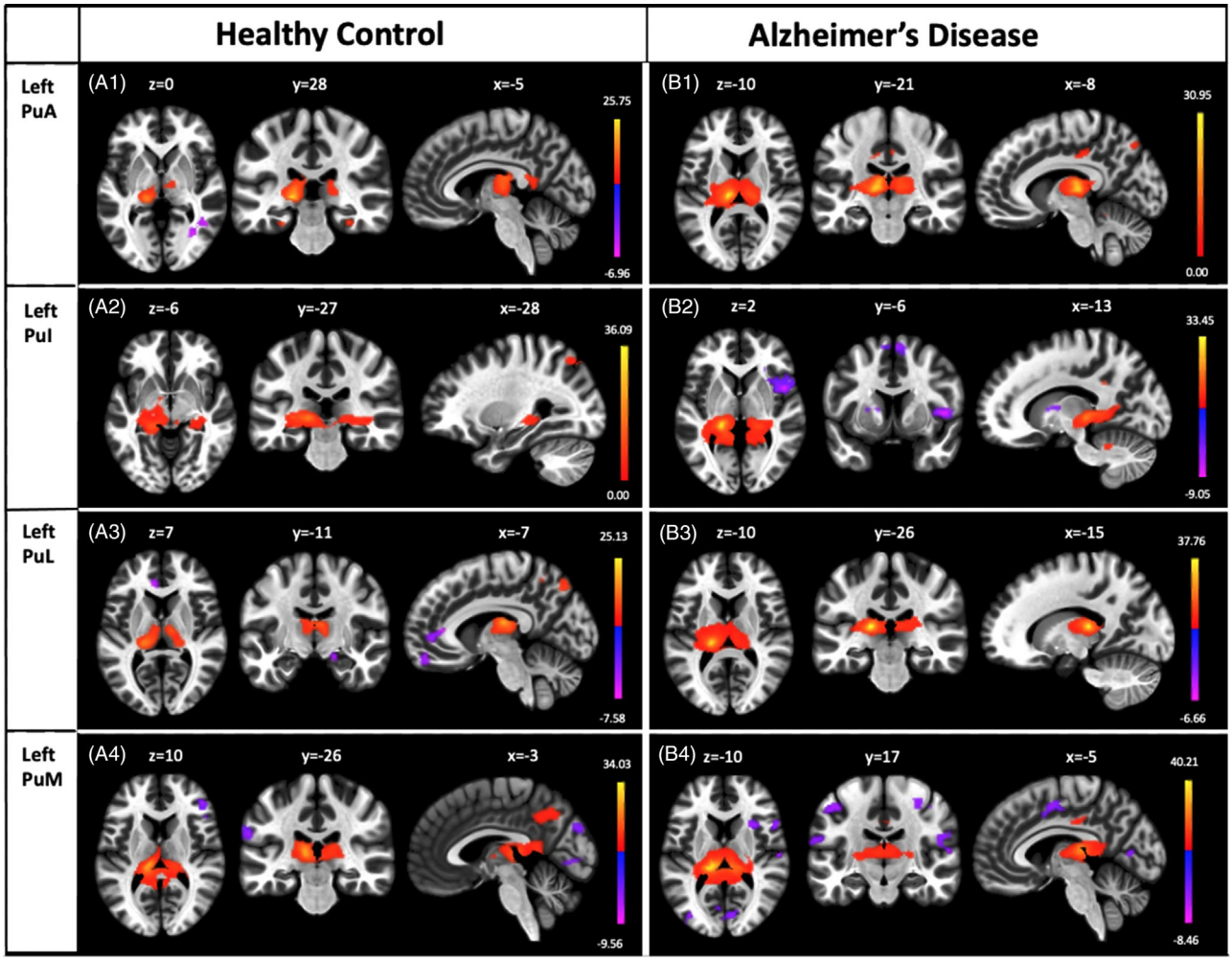

FIGURE 3 The mean group resting state functional connectivity map of left PuA, PuI, PuL, PuM seeds are shown, respectively, in A1, A2, A3, A4 for healthy controls and in B1, B2, B3, B4 for the Alzheimer's disease group. All maps are family-wise error corrected at $P < 0.00625$ with a minimum of 10 voxels for each cluster. The slice labels are in Montreal Neurological Institute standard space. The color bar represents *t* statistics. The red patches show the functionally positive correlated areas with pulvinar seeds in both groups, and the purple patches show the functionally negative correlated areas with pulvinar seeds in both groups. The regions shown in this figure are described in Table 1. PuA, anterior pulvinar; PuI, inferior pulvinar; PuL, lateral pulvinar; PuM, medial pulvinar

as first-level covariates in the denoising procedure. The structural and functional images were registered after the scrubbing. Consequently, low-resolution functional images were aligned to the plane of high-resolution structural images and made ready for the normalization step. Preprocessing using the tissue probability maps normalized structural images into GM, white matter (WM), and cerebrospinal fluid (CSF). The functional and anatomical images were resliced to $2 \times 2 \times 2$ mm voxels and normalized into the Montreal Neurological Institute (MNI) space during normalization. Functional data were smoothed with an 8-mm full width at half maximum (FWHM) Gaussian kernel. In the denoising step, functional images were band-pass filtered to 0.008–0.09 Hz to reduce the effect of noise after preprocessing. The six motion parameters and their first-order derivatives were then regressed, as well as the signals collected from WM, CSF as an anatomical component-based noise correction process (aCompCor), and the confounding factors deriving from the resting condition.[48] The eight pulvinar subdivision regions of interest (ROIs), obtained through FreeSurfer thalamic segmentation, were added to the CONN toolbox in seed-to-voxel analysis. In the first-level analysis, the average time series of all ROIs were extracted for the BOLD time series, and the correlation coefficients between the BOLD time series obtained from each brain voxel were computed. For statistical analysis, these correlation coefficients were then z-transformed using the Fisher transformation. All ROI *z*-values were compared between the two groups using analysis of variance (ANOVA) at the second level, with $p_{unc} < 0.001$ at the voxel level and family-wise error (FWE) adjusted $p_{FWE} < 0.05$ at the cluster level. The Bonferroni-corrected results were given after *P*-values were corrected for multiple comparisons (pFWE-BC < 0.00625).

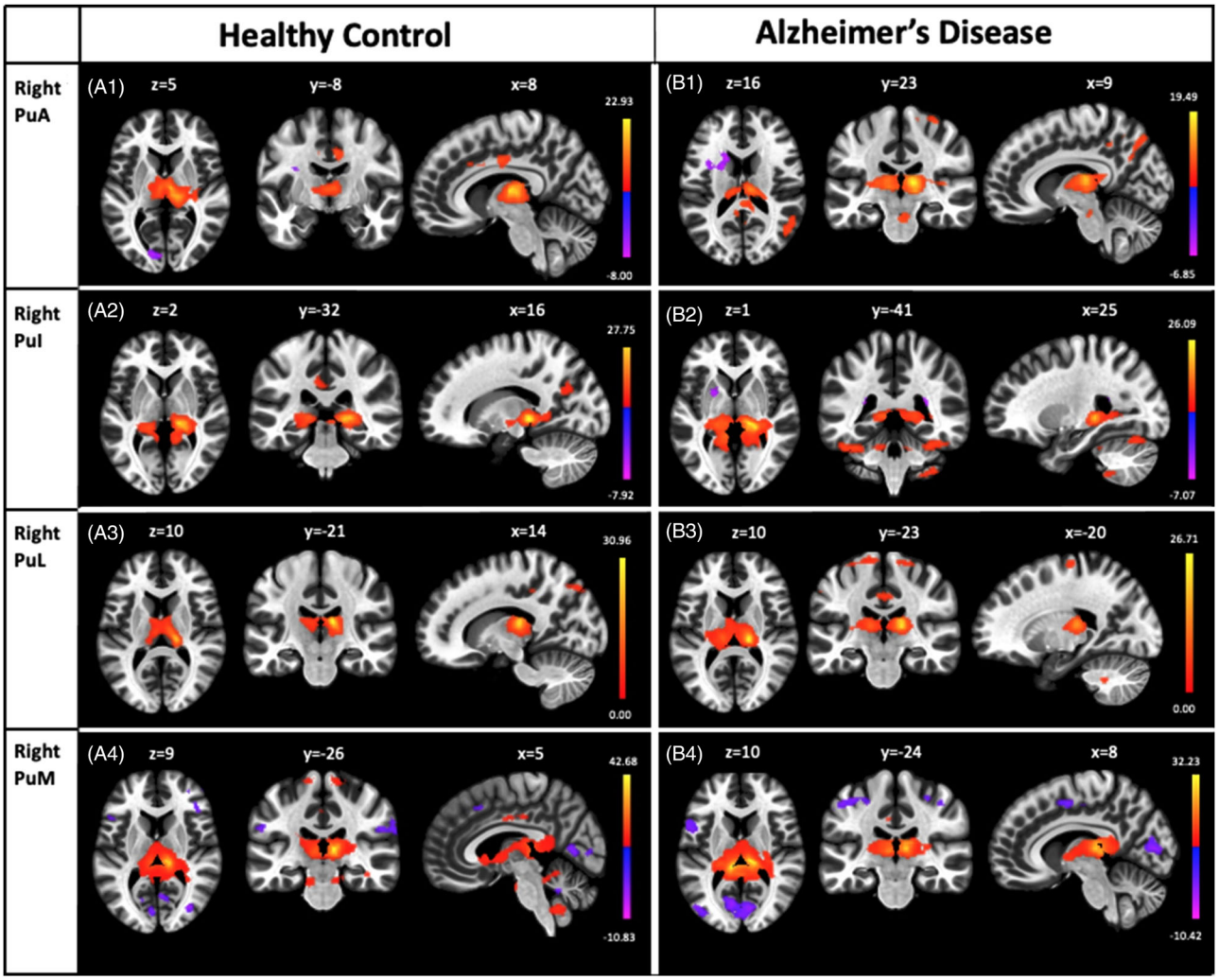

FIGURE 4 The mean group resting state functional connectivity map of right PuA, PuI, PuL, PuM seeds are shown, respectively, in A1, A2, A3, A4 for healthy controls and in B1, B2, B3, B4 for the Alzheimer's disease group. All maps are family-wise error corrected at $P < 0.00625$ with a minimum of 10 voxels for each cluster. The slice labels are in Montreal Neurological Institute standard space. The color bar represents *t* statistics. The red patches show the functionally positive correlated areas with pulvinar seeds in both groups, and the purple patches show the functionally negative correlated areas with pulvinar seeds in both groups. The regions shown in this figure are described in Table 2. PuA, anterior pulvinar; PuI, inferior pulvinar; PuL, lateral pulvinar; PuM, medial pulvinar

2.4 | Structural processing

The Computational Anatomy Toolbox (CAT12, http://dbm.neuro.uni-jena.de/cat/), an extension toolbox of Statistical Parametric Mapping software (SPM12, http://www.fil.ion.ucl.ac.uk/spm/software/) in MATLAB (20b) was used to process the high-resolution 3D T1-weighted images for voxel based-morphometry (VBM) analysis.[48] The high-resolution T1 images were affine registered, corrected for bias-field inhomogeneities, and segmented into GM, WM, and CSF tissues according to the MNI template space. In addition, total intracranial volume (TIV) was calculated to correct for different brain sizes and volumes. Finally, the GM images were smoothed using a Gaussian filter (8 mm full-width half-maximum, FWHM) via the standard SPM module "Smooth" to increase the signal-to-noise ratio. A quality check, the homogeneity of the GM tissues, was assessed after the preprocessing. Group differences in pulvinar and thalamus volumes were compared by one-way ANOVAs. The subjects' age and TIVs in the design matrix were added as covariates because certain researchers showed that the age and TIV of subjects had an impact on the VBM results.[49] To address multiple comparisons, all statistical maps were reported after correction as voxel-level threshold: uncorrected $P < 0.001$, cluster level threshold: FWE $P < 0.05$.

2.5 | Thalamus segmentation for pulvinar seeds

We performed autonomic thalamus segmentation using FreeSurfer software (http://surfer.nmr. mgh.harvard.edu/) to create the seeds in the current study. The thalamic nuclei of MNI 2 mm standard space were automatically segmented using the "recon-all" function.[50] The

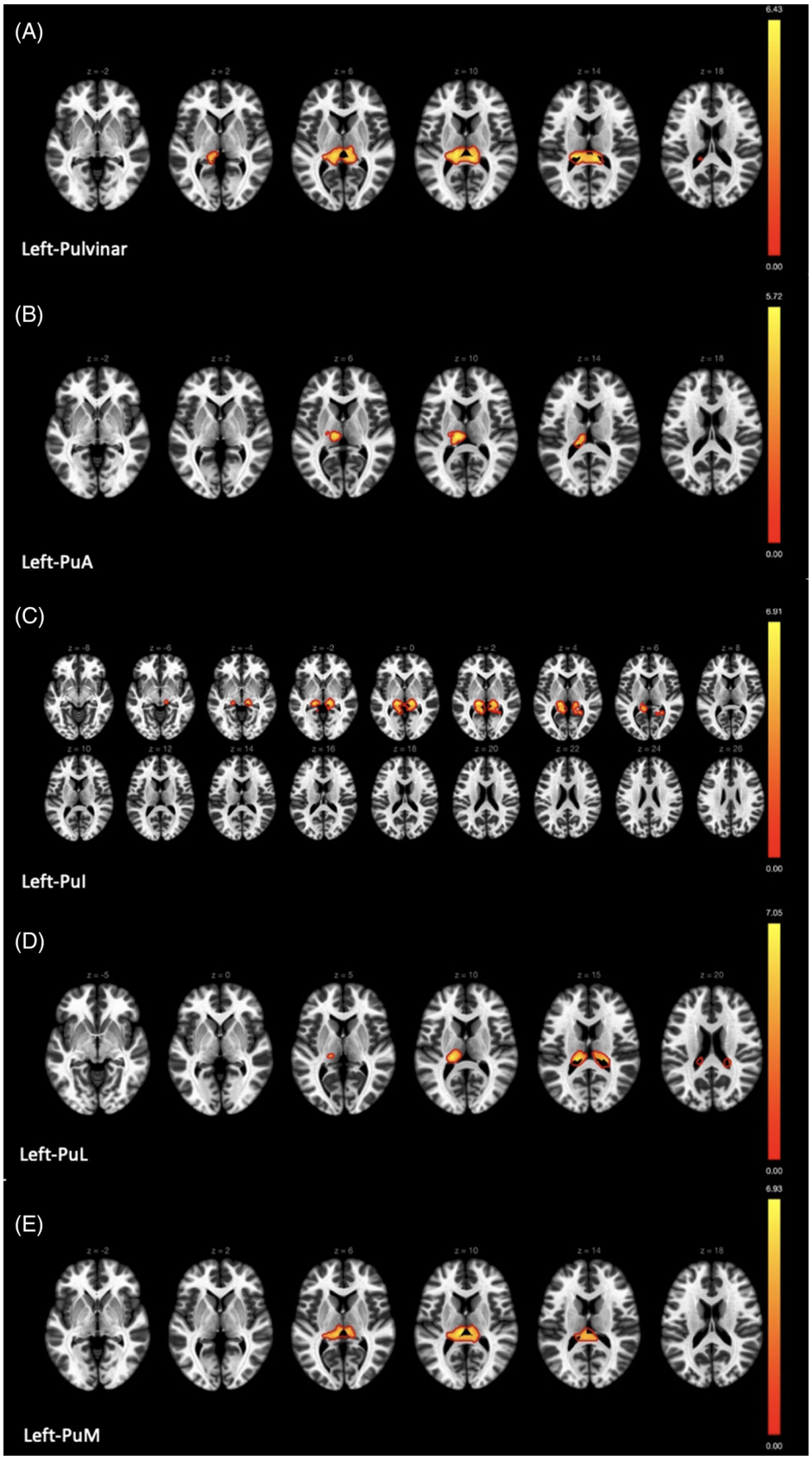

FIGURE 5 Group connectivity differences between groups for left pulvinar, PuA, PuI, PuL, PuM in A, B, C, D, E, respectively. *P*-value measures the difference between groups by one-way analyses of covariance ($P < 0.001$ voxel and *P*-FWE < 0.00625 at cluster level). FWE, family-wise error; PuA, anterior pulvinar; PuI, inferior pulvinar; PuL, lateral pulvinar; PuM, medial pulvinar

Alzheimer's & Dementia®
THE JOURNAL OF THE ALZHEIMER'S ASSOCIATION

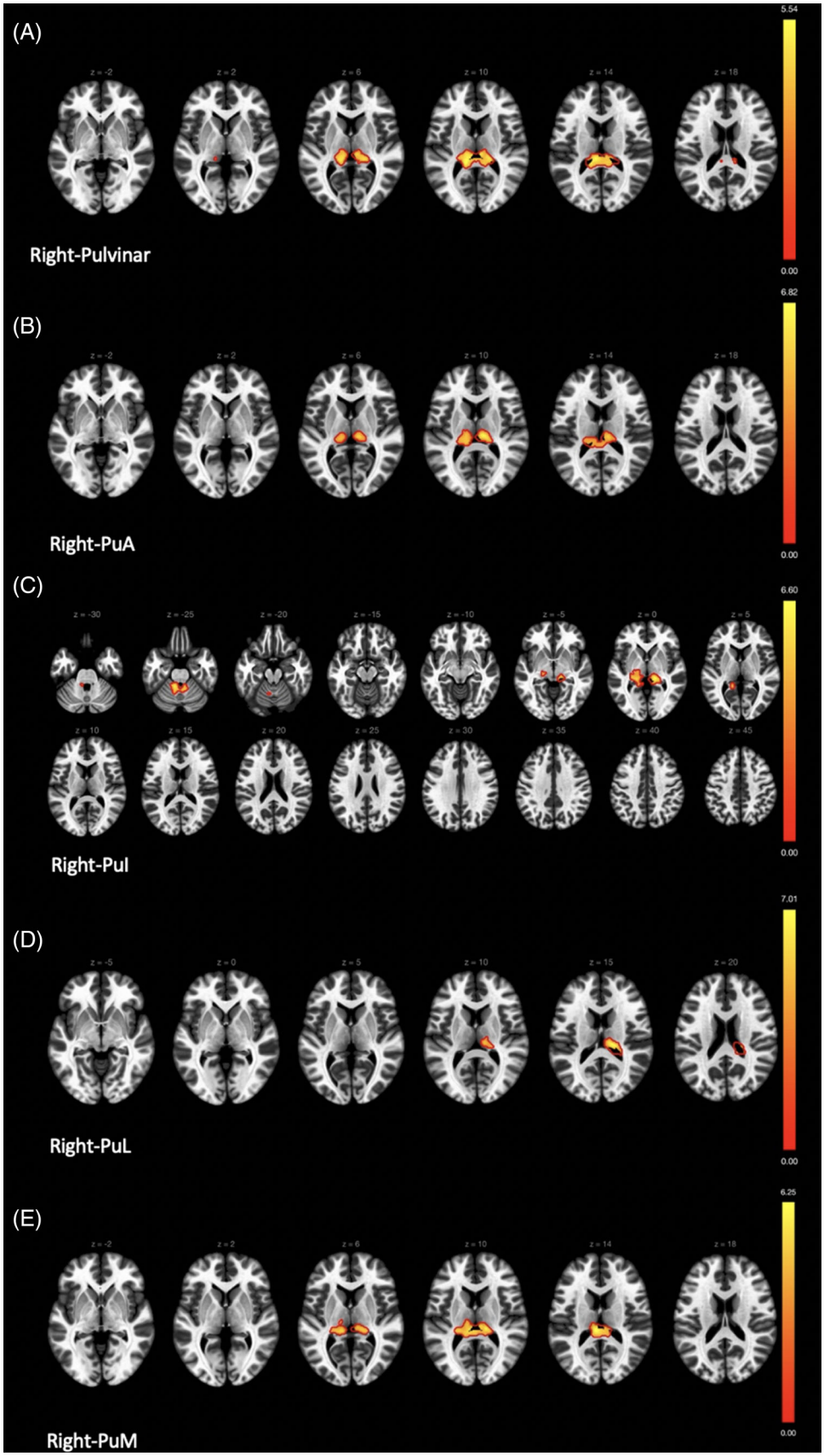

FIGURE 6 Group connectivity differences between groups for right pulvinar, PuA, PuI, PuL, PuM in A, B, C, D, E, respectively. *P*-value measures the difference between groups by one-way analyses of covariance ($P < 0.001$ voxel and P-FWE < 0.00625 at cluster level). FWE, family-wise error; PuA, anterior pulvinar; PuI, inferior pulvinar; PuL, lateral pulvinar; PuM, medial pulvinar

TABLE 3 The functional connectivity differences between groups

	MNI coordinate	Region	Clusters size	FWE
Left-pulvinar	08, −34, 12	L-R thalamus L-hippocampus	1019	0.000000
L-PuA	−12, −22, 10	L-thalamus	203	0.004305
L-PuI	−16, −30, 02	L-thalamus, PCC, L-hippocampus	257	0.000319
	14, −28, 00	R-thalamus, PCC, R-hippocampus Brainstem	216	0.000392
L-PuL	−18, −28, 00	L-thalamus	196	0.000331
L-PuM	−08, −26, 10	L-R thalamus	355	0.000002
Right-pulvinar	−12, −34, 10	L-R thalamus	814	0.000000
R-PuA	10, −22, 10	L-R thalamus	310	0.000008
R-PuI	−18, −30, 00	L-thalamus, PCC, L-hippocampus	152	0.002169
	−10, −44, −24	Brainstem L-cerebellum	81	0.002223
	14, −30, 00	R-thalamus, R-hippocampus	200	0.003558
R-PuL	16, −26, 16	R-thalamus	141	0.000726
R-PuM	−06, −30, 14	L-R thalamus	316	0.000002

Notes: *P*-value assesses the difference between groups by one-way analyses of covariance ($P < 0.001$ voxel and P-FWE < 0.00625 at cluster level). The related regions showed stronger connectivity in the healthy group compared to the AD group.
Abbreviations: AD, Alzheimer's disease; FWE, family-wise error; PuA, anterior pulvinar; PuI, inferior pulvinar; PuL, lateral pulvinar; PuM, medial pulvinar

PuA, PuI, PuL, and PuM in each hemisphere were selected as seeds after the thalamus segmentation (Figure 2). The guidelines provided by Williams were followed to convert the seeds from FreeSurfer format (.mgh/.mgz) to Nifti (.nii/.nii.gz) format.[51]

2.5.1 | Results

The average age of the AD group is 70.31 ± 7.8 years (nine females and seven males); the average age of the healthy control group is 60.26 ± 9.37 years (nine females and six males). We found no differences between groups in terms of sex in the two groups ($P > 0.005$). Healthy subjects without any history of neurological diseases had higher MMSE (mean: 28) scores. On the other hand, patients with AD who had mild to severe AD symptoms had lower MMSE (mean: 17) scores. The AD group had statistically significant higher ages ($P < 0.005$) and lower cognitive performance according to the scores in the MMSE compared to the healthy group ($P < 0.001$). Based on this significant clinical data we included the mean age and MMSE as covariates in the functional connectivity and VBM analysis to control for covariates by group interactions (one-way analyses of covariance and post hoc [Bonferroni] tests), which gave the following results.

2.5.2 | Within-group functional connectivity

We found extensive functional connectivity of the pulvinar in healthy controls. Interestingly, the regions demonstrating functional connectivity with the pulvinar were mainly similar to AD. We found functional connectivity between the left pulvinar nucleus and the thalamus, hippocampus, amygdala, cerebellum, and cortical areas, including the precuneus cortex, superior parietal lobule, supramarginal gyrus, fusiform cortex, inferior temporal gyrus, middle temporal gyrus, posterior parahippocampal gyrus, lateral occipital cortex, lingual gyrus, intracalcarine cortex, frontal medial cortex, precentral gyrus, middle frontal gyrus, superior frontal gyrus, anterior cingulate cortex, posterior cingulate cortex, and paracingulate gyrus in healthy controls. In the AD group, the left pulvinar nucleus exhibited connectivity to the thalamus, putamen, hippocampus, cerebellum, and cortical areas including inferior frontal gyrus, middle frontal gyrus, superior frontal gyrus, supplementary motor cortex, precentral cortex, fusiform cortex, inferior temporal gyrus, precuneus cortex, postcentral gyrus, lingual gyrus, intracalcarine cortex, supra calcarine cortex, insular cortex, anterior cingulate cortex, posterior cingulate cortex (Table 1 and Figure 3). We identified functional connectivity of the right pulvinar nucleus with the thalamus, hippocampus, brainstem, cerebellum, and cortical

TABLE 4 The VBM analysis between groups

	Healthy controls		Alzheimer's disease		Mean differences (*P*-value)
	Mean %	SD %	Mean %	SD %	Healthy control > Alzheimer's disease
Right pulvinar	0.82069	0.084392	0.63339	0.097854	**0.000
Left pulvinar	0.64909	0.067201	0.50084	0.061259	**0.000
Right thalamus	4.92291	0.281830	3.97637	0.710437	**0.000
Left thalamus	4.82235	0.276868	3.91705	0.756019	**0.000

Abbreviations: L, left; R, right; SD, standard deviation; VBM, voxel-based morphometry.
**$P < 0.01$.

areas, including angular gyrus, postcentral gyrus, precuneus cortex, supramarginal gyrus, superior parietal lobule, fusiform cortex, intracalcarine cortex, lingual gyrus, inferior frontal gyrus, middle frontal gyrus, precentral gyrus, insular cortex, anterior cingulate cortex, posterior cingulate cortex in healthy controls. In the AD group, the right pulvinar nucleus exhibited connectivity to the thalamus, putamen, pallidum, caudate, hippocampus, cerebellum, and cortical areas including angular gyrus, precuneus cortex, postcentral gyrus, supramarginal gyrus, superior parietal lobule, fusiform cortex, intracalcarine cortex, lateral occipital cortex, lingual gyrus, middle temporal gyrus, precentral gyrus, supplementary motor cortex, insula cortex, posterior cingulate cortex (Table 2 and Figure 4; $P < 0.00625$ p-FEW corrected).

2.5.3 | Between-groups functional connectivity

The present study found a significant correlation between group differences in functional connectivity of the pulvinar and its subdivisions. In particular, the stronger connectivity was found in the left pulvinar with bilateral thalamus and left hippocampus; PuA with left thalamus; left PuI with bilateral thalamus, bilateral hippocampus, and posterior cingulate cortex; left PuL with the left thalamus; left PuM with bilateral thalamus; right pulvinar with bilateral thalamus; right PuA with bilateral thalamus; right PuI with bilateral thalamus, bilateral hippocampus, left brainstem, and posterior cingulate cortex; right PuL with right thalamus; right PuM with bilateral thalamus in healthy controls group than in the AD group (Table 3 and Figures 5 and 6; $P < 0.00625$ p-FWE corrected).

2.5.4 | Voxel-based morphometry analysis

The mean volumes of pulvinar and whole thalamus are shown for the two study groups in Table 4. In the VBM analysis between patients with AD and healthy controls, the total volume of both pulvinars in patients with AD was significantly smaller compared to the healthy controls ($P < 0.000$). Furthermore, whole thalamus volume in each hemisphere was also significantly reduced in the AD group compared to the healthy controls ($P < 0.000$).

ACKNOWLEDGMENTS

The authors of this work are grateful to Istanbul Medipol University, Research Institute for Health and Technologies (SABITA). Additionally, we thank Carl Nino Rossini for the English advice and corrections.

CONFLICTS OF INTEREST

The authors of this manuscript declare no relationships with any companies, whose products or services may be related to the subject matter of the article. Author disclosures are available in the supporting information.

ORCID

Burak Yulug https://orcid.org/0000-0002-9704-6173

REFERENCES

1. Chapleau M, Aldebert J, Montembeault M, Brambati SM. Atrophy in Alzheimer's disease and semantic dementia: an ALE meta-analysis of voxel-based morphometry studies. *J Alzheimers Dis*. 2016;54(3):941-955. https://doi.org/10.3233/JAD-160382
2. Dicks E, Vermunt L, van der Flier WM, et al. Modeling grey matter atrophy as a function of time, aging or cognitive decline show different anatomical patterns in Alzheimer's disease. *Neuroimage Clin*. 2019;22(March):101786. https://doi.org/10.1016/j.nicl.2019.101786
3. Kang SW, Jeon S, Yoo HS, et al. Effects of Lewy body disease and Alzheimer disease on brain atrophy and cognitive dysfunction. *Neurology*. 2019;92(17):E2015-E2026. https://doi.org/10.1212/WNL.0000000000007373
4. Kunst J, Marecek R, Klobusiakova P, et al. Patterns of grey matter atrophy at different stages of Parkinson's and Alzheimer's diseases and relation to cognition. *Brain Topogr*. 2019;32(1):142-160. https://doi.org/10.1007/s10548-018-0675-2
5. Kuljis RO. Lesions in the pulvinar in patients with Alzheimer's disease. *J Neuropathol Exp Neurol*. 1994;53(2):202-211. https://doi.org/10.1097/00005072-199403000-00012
6. Insel PS, Mormino EC, Aisen PS, Thompson WK, Donohue MC. Neuroanatomical spread of amyloid β and tau in Alzheimer's disease: implications for primary prevention. *Brain Commun*. 2020;2(1):1-11. https://doi.org/10.1093/braincomms/fcaa007
7. Halassa MM, Kastner S. Thalamic functions in distributed cognitive control. *Nat Neurosci*. 2017;20(12):1669-1679. https://doi.org/10.1038/s41593-017-0020-1
8. Aggleton JP, Pralus A, Nelson AJD, Hornberger M. Thalamic pathology and memory loss in early Alzheimer's disease: moving the focus from the medial temporal lobe to Papez circuit. *Brain*. 2016;139(7):1877-1890. https://doi.org/10.1093/brain/aww083

9. Michael D, Rugg Danielle R, King Center. Ventral lateral parietal cortex and episodic memory retrieval. *Physiol Behav*. 2017;176(5):139-148. https://doi.org/10.1016/j.cortex.2017.07.012.Ventral
10. Kaas JH, Lyon DC. Pulvinar contributions to the dorsal and ventral streams of visual processing in primates. *Brain Res Rev*. 2007;55(2):285-296. https://doi.org/10.1016/j.brainresrev.2007.02.008
11. Lakatos P, O'Connell MN, Barczak A. Pondering the Pulvinar. *Neuron*. 2016;89(1):5-7. https://doi.org/10.1016/j.neuron.2015.12.022
12. Lyon DC, Jain N, Kaas JH. The visual pulvinar in tree shrews II. Projections of four nuclei to areas of visual cortex. *J Comp Neurol*. 2003;467(4):607-627. https://doi.org/10.1002/cne.10940
13. Olszewski J. *The Thalamus of the Macaca Mulatta*. Kerger; 1952. https://doi.org/10.1002/cne.901000312
14. Sheremata SL, Somers DC, Shomstein S. Visual short-term memory activity in parietal lobe reflects cognitive processes beyond attentional selection. *J Neurosci*. 2018;38(6):1511-1519. https://doi.org/10.1523/JNEUROSCI.1716-17.2017
15. Karunakaran KD, Yuan R, He J, et al. Resting-state functional connectivity of the thalamus in complete spinal cord injury. *Neurorehabil Neural Repair*. 2020;34(2):122-133. https://doi.org/10.1177/1545968319893299
16. Saalmann YB, Kastner S. Cognitive and perceptual functions of the visual thalamus. *Neuron*. 2011;71(2):209-223. https://doi.org/10.1016/j.neuron.2011.06.027.Cognitive
17. Romanski LM, Giguere M, Bates JF, Goldman-Rakic PS. Topographic organization of medial pulvinar connections with the prefrontal cortex in the rhesus monkey. *J Comp Neurol*. 1997;379(3):313-332. https://doi.org/10.1002/(SICI)1096-9861(19970317)379
18. Arend I, Henik A, Okon-Singer H. Dissociating emotion and attention functions in the pulvinar nucleus of the thalamus. *Neuropsychology*. 2015;29(2):191-196. https://doi.org/10.1037/neu0000139
19. Koizumi A, Zhan M, Ban H, et al. Threat anticipation in pulvinar and in superficial layers of primary visual cortex (V1). Evidence from layer-specific ultra-high field 7T fMRI. *eNeuro*. 2019;6(6):1-11. https://doi.org/10.1523/ENEURO.0429-19.2019
20. Guedj C, Vuilleumier P. Functional connectivity fingerprints of the human pulvinar: decoding its role in cognition. *Neuroimage*. 2020;221:117162. https://doi.org/10.1016/j.neuroimage.2020.117162
21. Leh SE, Chakravarty MM, Ptito A. The connectivity of the human pulvinar: a diffusion tensor imaging tractography study. *Int J Biomed Imaging*. 2008;789539. https://doi.org/10.1155/2008/789539
22. Kastner S, O'Connor DH, Fukui MM, Fehd HM, Herwig U, Pinsk MA. Functional imaging of the human lateral geniculate nucleus and pulvinar. *J Neurophysiol*. 2004;91(1):438-448. https://doi.org/10.1152/jn.00553.2003
23. Homman-Ludiye J, Mundinano IC, Kwan WC, Bourne JA. Extensive connectivity between the medial pulvinar and the cortex revealed in the marmoset monkey. *Cerebral Cortex*. 2020;30(3):1797-1812. https://doi.org/10.1093/cercor/bhz203
24. Bourgeois A, Guedj C, Carrera E, Vuilleumier P. Pulvino-cortical interaction: an integrative role in the control of attention. *Neurosci Biobehav Rev*. 2020;111:104-113. https://doi.org/10.1016/j.neubiorev.2020.01.005
25. Baldwin MaryKL, Balaram JHKaas Pooja. The evolution and functions of nuclei of the visual pulvinar in primates. *J Comp Neurol*. 2017;525(15):3207-3226. https://doi.org/10.1002/cne
26. Homman-Ludiye J, Bourne JA. The medial pulvinar: function, origin and association with neurodevelopmental disorders. *J Anat*. 2019;235(3):507-520. https://doi.org/10.1111/joa.12932
27. Benarroch EE. Pulvinar: Associative role in cortical function and clinical correlations. *Neurology*. 2015;84(7):738-747. https://doi.org/10.1212/WNL.0000000000001276
28. Danziger S, Ward R, Owen V, Rafal R. Contributions of the human pulvinar to linking vision and action. *Cogn Affect Behav Neurosci*. 2004;4(1):89-99. https://doi.org/10.3758/CABN.4.1.89
29. Danziger S, Ward R, Owen V, Rafal R. The effects of unilateral pulvinar damage in humans on reflexive orienting and filtering of irrelevant information. *Behav Neurol*. 2001;13(3-4):95-104. https://doi.org/10.1155/2002/917570
30. Wester K, Irvine DRF, Hugdahl K. Auditory laterality and attentional deficits after thalamic haemorrhage. *J Neurol*. 2001;248(8):676-83. https://doi.org/10.1007/s004150170113
31. Arend I, Rafal R, Ward R. Spatial and temporal deficits are regionally dissociable in patients with pulvinar lesions. *Brain*. 2008;131(8):2140-2152. https://doi.org/10.1093/brain/awn135
32. Wilke M, Schneider L, Dominguez-Vargas AU, et al. Reach and grasp deficits following damage to the dorsal pulvinar. *Cortex*. 2018;99:135-149. https://doi.org/10.1016/j.cortex.2017.10.011
33. Bridge H, Leopold DA, Bourne JA. Adaptive pulvinar circuitry supports visual cognition. *Trends Cogn Sci*. 2016;20(2):146-157. https://doi.org/10.1016/j.tics.2015.10.003
34. Erskine D, Thomas AJ, Attems J, et al. Specific patterns of neuronal loss in the pulvinar nucleus in dementia with Lewy bodies. *Movement Disorders*. 2017;32(3):414-422. https://doi.org/10.1002/mds.26887
35. Tak K, Lee S, Choi E, et al. Magnetic resonance imaging texture of medial pulvinar in dementia with Lewy bodies. *Dement Geriatr Cogn Disord*. 2020;49(1):8-15. https://doi.org/10.1159/000506798
36. Pardilla-Delgado E, Torrico-Teave H, Sanchez JS, et al. Associations between subregional thalamic volume and brain pathology in autosomal dominant Alzheimer's disease. *Brain Commun*. 2021;3(2):fcab101. https://doi.org/10.1093/BRAINCOMMS/FCAB101
37. Mufson EJ, Mesulam MM. Thalamic connections of the insula in the rhesus monkey and comments on the paralimbic connectivity of the medial pulvinar nucleus. *J Comp Neurol*. 1984;227(1):109-120. https://doi.org/10.1002/CNE.902270112
38. Cotton PL, Smith AT. Contralateral visual hemifield representations in the human pulvinar nucleus. *J Neurophysiol*. 2007;98(3):1600-1609. https://doi.org/10.1152/JN.00419.2007
39. Baleydier C, Morel A. Segregated thalamocortical pathways to inferior parietal and inferotemporal cortex in macaque monkey. *Vis Neurosci*. 1992;8(5):391-405. https://doi.org/10.1017/S0952523800004922
40. Van De Mortel LA, Thomas RM, Van Wingen GA. Grey matter loss at different stages of cognitive decline: a role for the thalamus in developing Alzheimer's disease. *Journal of Alzheimers Dis*. 2021;83(2):705-720. https://doi.org/10.3233/JAD-210173
41. Zhang H, Trollor JN, Wen W, et al. Grey matter atrophy of basal forebrain and hippocampus in mild cognitive impairment. *J Neurol Neurosurg Psychiatry*. 2011;82(5):487-493. https://doi.org/10.1136/jnnp.2010.217133
42. Valdés Hernández MC, Clark R, Wang SH, et al. The striatum, the hippocampus, and short-term memory binding: volumetric analysis of the subcortical grey matter's role in mild cognitive impairment. *Neuroimage Clin*. 2020;25:102158. https://doi.org/10.1016/j.nicl.2019.102158
43. Whitfield-Gabrieli S, Nieto-Castanon A. Conn: A functional connectivity toolbox for correlated and anticorrelated brain networks. *Brain Connect*. 2012;2(3):125-141. https://doi.org/10.1089/brain.2012.0073
44. Power JD, Barnes KA, Snyder AZ, Schlaggar BL, Petersen SE. Spurious but systematic correlations in functional connectivity MRI networks arise from subject motion. *Neuroimage*. 2012;59(3):2142-2154. https://doi.org/10.1016/j.neuroimage.2011.10.018
45. van Dijk KRA, Sabuncu MR, Buckner RL. The influence of head motion on intrinsic functional connectivity MRI. *Neuroimage*. 2012;59(1):431-438. https://doi.org/10.1016/j.neuroimage.2011.07.044

46. Mazaika PK, Hoeft F, Glover GH, Reiss AL. Methods and software for fMRI analysis of clinical subjects. *Neuroimage*. 2009;47:S58. https://doi.org/10.1016/s1053-8119(09)70238-1
47. Behzadi Y, Restom K, Liau J, Liu TT. A component based noise correction method (CompCor) for BOLD and perfusion based fMRI. *Neuroimage*. 2007;37(1):90-101. https://doi.org/10.1016/j.neuroimage.2007.04.042
48. Gaser C, Dahnke R. CAT-a computational anatomy toolbox for the analysis of structural MRI data. *Hbm*. 2016;2016:336-348. https://doi.org/10.1101/2022.06.11.495736
49. Peelle JE, Cusack R, Henson RNA. Adjusting for global effects in voxel-based morphometry: gray matter decline in normal aging. *Neuroimage*. 2012;60(2):1503-1516. https://doi.org/10.1016/j.neuroimage.2011.12.086
50. Iglesias JE, Insausti R, Lerma-Usabiaga G, et al. A probabilistic atlas of the human thalamic nuclei combining ex vivo MRI and histology. *Neuroimage*. 2018;183(June):314-326. https://doi.org/10.1016/j.neuroimage.2018.08.012
51. Creating anatomical masks with Freesurfer Thalamic segmentation. https://neurobren.com/freesurfer-masks/

SUPPORTING INFORMATION

Additional supporting information can be found online in the Supporting Information section at the end of this article.

How to cite this article: Velioglu HA, Ayyildiz B, Ayyildiz S, et al. A structural and resting-state functional connectivity investigation of the pulvinar in elderly individuals and Alzheimer's disease patients. *Alzheimer's Dement*. 2023;19:2774–2789. https://doi.org/10.1002/alz.12850